*J. Fluid Mech.* (1994), *vol.* 275, *pp.* 301–321



# On narrow V-like ship wakes

By DAIFANG GU† AND O. M. PHILLIPS

Department of Earth and Planetary Sciences, The Johns Hopkins University, Baltimore, MD 21218, USA

(Received 2 February 1992 and in revised form 4 April 1994)

This paper is concerned with the generation of short gravity waves and their radiation from the outer edge of the turbulent boundary layer and wake of a ship. They arise primarily near the ship's stern. The wave spectrum in the direction of wavenumber vector at an angle $(90°-\delta)$ to the ship's track is:

$$\Phi_\delta(\omega) = \Psi\left(\frac{UT_d}{2l}, \frac{U\sin\delta}{c_g}, \frac{R}{UT_d}\right)\frac{1}{k_0 R}\frac{2l\omega^2}{g^2}\Upsilon\left(0, \frac{\pi}{l}; 0, \omega\right),$$

where $\Psi$ is dimensionless and a function of three dimensionless parameters. $\Upsilon$ is the spectrum of the oscillating motion at the boundary, $U$ the ship speed, $T_d$ the decay timescale of the oscillating motion, $2l$ the lengthscale of the eddies, and $R$ the distance away from the boundary along the wavenumber vector. Generally, $\Phi_\delta$ has large values near $\delta = 0$ and small values at large $\delta$; it behaves as $1/R$ at distances not far from the ship, then may vary slower than $1/R$ at intermediate distances, and finally behaves as $1/R$ again at distances far from the ship. These are consistent with the pattern found in SAR images of narrow V-like ship wakes. The method developed here is also applicable to various problems of surface wave generation by turbulence in water.

## 1. Introduction

Ship waves have long been the interest of fluid dynamics. The classical Kelvin wave pattern, which originates from a point impulse moving at constant velocity along the surface of the water, consists of two kinds of waves, transverse and divergent, and is confined between two lines with half angle 19.5°. Recently, however, satellite and aircraft images of the sea surface, using Synthetic Aperture Radar, have revealed the existence of a narrow V-like wake extending as far as 20 km behind surface ships with a half angle between 2° and 3° (Shemdin 1987; Munk, Scully-Power & Zachariasen 1987). The length of such arms in general depends on the sea state, and the half angle varies from ship to ship and depends on ship speed and radar wavelength. This new discovery was surprising and has sparked considerable speculation. It must be kept in mind that the radar return from the sea surface to first order is the result of Bragg backscattering which selects a single wavenumber of the water surface configuration pointing in the same direction as the radar does. For the SEASAT SAR, the surface-wavelength selected by Bragg backscattering is about 30 cm. It was found that these surface-waves are not part of the Kelvin wake (Munk *et al.* 1987). In the Kelvin wake, such short wavelengths occur only within the divergent wave system and appear at rather small wake angle, but the direction which is proper for backscatter in one bright arm will not be proper for the other arm: only one arm would be visible to the radar.

† Present address: Program in Atmospheric and Oceanic Sciences, PO Box CN710, Sayre Hall, Princeton University, Princeton, NJ 08544-0710, USA.

FIGURE 1. A turbulent jet behind ship *Bay Lady* generated by propeller. Waves generated and radiated away by the jet are perceivable along the edge of the jet.

One supposition was that they are associated with ship-generated internal waves at the thermocline. Internal waves in general have smaller phase speeds than surface waves and propagate away from the axis of the ship, and the wake angle, which is proportional to the ratio of the internal wave phase speed to the ship speed, is smaller than that of the Kelvin wake. Modulation of short surface waves by the strain of internal waves can cause modulation of radar backscatter. Further studies showed however, that, the predicted radar backscatter modulation derived from internal wave modulation with a mixed layer depth of 100 m or so is one or two orders of magnitude smaller than what has been observed, so the internal waves may not be relevant to narrow V-like ship wakes (Shemdin 1987), at least under mild wind condition (Lyden *et al.* 1988). Another mechanism that has been proposed is that V-like wakes are mainly generated by incoherent point sources behind the ship (Munk *et al.* 1987). This is a very simple model and is in the spirit of this investigation. Figure 4 in his paper which was taken 500 m behind the ship shows clearly that waves are radiating from the incoherent point sources. However, we know that the strongest turbulent disturbances are located just behind the ship, and it may have a strong coherent structure. As time goes on, the small-scale disturbances in the turbulent wake die away, leaving behind a large-scale more or less coherent structure in the wake.

To clarify the generation mechanism, we made some observations of ship wakes under mild wind condition (less than 3 m $s^{-1}$). We found the ship wakes consist of two regions: one is the small defect wake generated by the ship's hull and full of swirling eddies, and the other is a strong turbulent jet generated by the propeller running through the middle of the small defect wake (figure 1). The structure, intensity, and the mean velocity of the jet's eddies depend on the state of the ship (such as ship speed, geometry, and its course), but the intensity of the flow disturbances strongly suggests that the dominant generating sources of the backscatter in the bright arms are located in the turbulent flow immediately astern. Small-scale waves are generated and radiated away by the oscillating boundary between the turbulence and the adjacent irrotational

FIGURE 2. Small-scale waves generated by a turbulent wake behind a ship. Note that the strongest waves last only for a few wave periods and each eddy acts like a single source of waves.

flow (figure 2). The purpose of this study is to investigate some characteristics of these waves generated by turbulence in ship wakes, in the hope of interpreting some of the unexplained features of the narrow V-like ship wakes.

The study of wave generation by floating bodies has long of an interest in fluid dynamics (Mei 1983), but so far no systematic theoretical work has been done for the generation of waves by turbulence. The well-established mathematical methods for wave generation by a floating body generally involve a complicated Green function (Michell 1898, Mei 1983) or an integral equation (Ursell 1966). These methods cannot be easily applied to the wave generation by turbulence, a more complicated process. In our present study, we find a Green function for the problem which leads to a relatively simple expression for the wave field in terms of normal velocities prescribed at the boundary so that wave generation by turbulence can be investigated analytically.

In §2, we will formulate the problem mathematically, give a general expression for the wave field in terms of the velocity distribution along the flat boundary, and discuss the characteristics of the waves generated by boundary disturbances in deep water. In §3, we will apply these results to the problem of narrow V-like ship wakes.

The phenomena of surface waves radiating away from turbulence occur in many other circumstances too, such as a turbulent stream entering a pool or a tank. Though in this paper we consider only the narrow V-like ship wakes, the principles and methods developed here can also be applied to these phenomena. Surface wave generation by turbulence is a difficult problem owing to its complexity. The model presented here is very idealized and we regard the present study as the first step towards understanding this difficult problem.

## 2. Wave generation by boundary disturbance

As a ship moves across the water surface, ship's turbulent wakes are generated, which consist of strong turbulent jets by propeller and a small defect wake; waves are radiated away from the edges of the jets and the defect wake (figures 1 and 2). This

suggests that waves may be generated by the velocity fluctuations at the edges of turbulent region.

It has been known for a long time that, for free turbulent flows such as jets, wakes, and boundary layers, there is a sharp but convoluted interface between the regions where the flow is turbulent and an external region of irrotational motion. If the surface-wave length is much greater than the thickness of the convolution region, the thickness of the convolution region can be neglected, and therefore the interface between irrotational and turbulent regions may be simplified as a local flat plane. Now we propose an idealized model of wave generation by turbulence: the turbulence and irrotational flows are separated by a vertical plane, and the velocity fluctuations in the plane induced by the turbulence give the specified normal velocity boundary conditions for the problem; it is this velocity distribution in the vertical plane that generates the gravity waves radiating away from the plane. The wave patterns and energy radiated away are solely determined by the characteristics of the boundary disturbances such as the intensity, the oscillating frequency, the lengthscale, and the advective velocity of the disturbance pattern. Thus, the problem of wave generation by turbulence has been simplified to a problem of wave generation by a prescribed but random boundary disturbance.

In this section, we first formulate the governing equation and find a Green's formula for the problem which leads to a relatively simple expression for the wave field in terms of normal velocities prescribed at the boundary so that wave generation by turbulence can be investigated analytically; then we investigate two special cases related to narrow V-like ship wake.

Let $z$ be the vertical coordinate with $x$ and $y$ as horizontal coordinates. The surface $z = 0$ is the undisturbed water surface, and $y = 0$ is the boundary between turbulence and irrotational flows – the control surface of the turbulence. The water depth is $h$. The normal velocity is prescribed at $y = 0$, and $y > 0$ is the irrotational region. Here we assume that the wave slope is small so that free-surface boundary conditions can be linearized. The governing equation and the boundary condition can be written as follows (Mei 1983):

$$\nabla^2\phi(t,x,y,z) = 0 \quad (-\infty < x < \infty, \quad y > 0, \quad -h < z \leqslant 0), \tag{1}$$

$$\frac{\partial\phi}{\partial t} + g\eta = 0 \quad \text{at } z = 0, \quad y > 0, \tag{2}$$

$$\frac{\partial\eta}{\partial t} = \frac{\partial\phi}{\partial z} \quad \text{at } z = 0, \quad y > 0, \tag{3}$$

$$\frac{\partial\phi}{\partial z} = 0 \quad \text{at } z = -h, \tag{4}$$

$$\frac{\partial\phi}{\partial y} = f(t,x,z) \quad \text{at } y = 0, \tag{5}$$

$$\phi \to 0 \quad \text{as } (x^2+y^2)^{1/2} \to \infty, \tag{6}$$

where $f(t,x,z)$ is the normal velocity prescribed at the boundary $y = 0$, $\phi$ is the velocity potential, and $\eta$ is the surface elevation. The flow is assumed to be at rest at time $t < 0$, and the disturbance at the plane $y = 0$ is switched on a time $t = 0$. The initial conditions for the problem are then

$$\phi(0,x,y,z) = 0, \tag{7}$$

$$\eta(0,x,y) = 0, \tag{8}$$

in the interior of the domain ($y > 0$).

Applying the Laplace transform

$$\bar{f}(s) = \int_0^\infty f(t)\,\mathrm{e}^{-st}\,\mathrm{d}t, \tag{9}$$

$$f(t) = \frac{1}{2\pi\mathrm{i}}\int_\Gamma \bar{f}(s)\,\mathrm{e}^{st}\,\mathrm{d}s, \tag{10}$$

to equations and boundary conditions (1)–(6) and noting the zero initial conditions for $\phi, \eta$, we have

$$\nabla^2\bar{\phi}(s,x,y,z) = 0 \quad (-\infty < x < \infty, \quad y > 0, \quad -h < z \leqslant 0), \tag{11}$$

$$\frac{\partial\bar{\phi}(s,x,y,0)}{\partial z} + \frac{s^2}{g}\bar{\phi}(s,x,y,0) = 0 \quad (z = 0, y > 0), \tag{12}$$

$$\frac{\partial\bar{\phi}(s,x,y,z)}{\partial z} = 0 \quad (z = -h), \tag{13}$$

$$\frac{\partial\bar{\phi}(s,x,y,z)}{\partial y} = \bar{f}(s,x,z) \quad (y = 0), \tag{14}$$

$$\bar{\phi}(s,x,y,z) \to 0 \quad ((x^2+y^2)^{1/2} \to \infty), \tag{15}$$

To solve the above equations, we first seek the Green function of the problem $G(s,x,y,z;x_0,y_0,z_0)$ which satisfies the following equations and boundary conditions:

$$\nabla^2 G = \delta(x-x_0)\,\delta(y-y_0)\,\delta(z-z_0) + \delta(x-x_0)\,\delta(y+y_0)\,\delta(z-z_0), \tag{16}$$

$$\frac{\partial G}{\partial z} + \frac{s^2}{g}G = 0 \quad \text{at } z = 0, \tag{17}$$

$$\frac{\partial G}{\partial z} = 0 \quad \text{as } z = -h, \tag{18}$$

$$\frac{\partial G}{\partial y}\Big|_{y=0} = 0, \tag{19}$$

$$G \to 0 \quad ((x^2+y^2)^{1/2} \to \infty). \tag{20}$$

Care has to be taken about the Neumann type of boundary condition at $y = 0$. In general, because of the Green's formula,

$$\iiint_{V_0} (u\nabla^2 v - v\nabla^2 u)\,\mathrm{d}V_0 = \iint_{S_0}\left(u\frac{\partial v}{\partial n} - v\frac{\partial u}{\partial n}\right)\mathrm{d}S_0, \tag{21}$$

the simplest allowable boundary condition for the Neumann type boundary condition is

$$\frac{\partial G}{\partial n} = \frac{1}{A}, \tag{22}$$

where $A$ is the area of the boundary. This is obtained by letting $u$ = constant and $v = G$. In our problem, however, we have prescribed that $\bar{\phi}$ goes to zero as distance $r_0 = (x^2+y^2)^{1/2}$ tends to infinity. In other words, if $\bar{\phi}$ is a constant in the entire domain, $\bar{\phi}$ must be zero. Therefore, Green's formula (21) is not violated here by imposing the boundary condition $(\partial G/\partial n)|_{y=0} = 0$, and (22) is not derivable from (21) any more.

Applying the Hankel transform to the governing equation and boundary conditions for $G$, noting that the mass flux coming out of the point sources at $(x_0, \pm y_0)$ is finite and that the radiation condition is

$$(kr_0)^{1/2}\left(\frac{\partial G}{\partial r_0} - ikG\right) \to 0 \quad \text{as } r_0 \to \infty,$$

we finally obtain the Green function of the problem (16)–(20):

$$G(s,x,y,z;x_0,y_0,z_0) = \frac{1}{2\pi}\int_0^\infty \frac{s^2\sinh kz_+ - gk\cosh kz_+}{s^2 + gk\tanh kh} \times \{J_0(kr') + J_0(kr'')\}\frac{\cosh k(z_- + h)}{\cosh kh}\,\mathrm{d}k, \quad (23)$$

where $r' = ((x-x_0)^2+(y-y_0)^2)^{1/2}$, $r'' = ((x-x_0)^2+(y+y_0)^2)^{1/2}$,

$$z_+ = \max(z, z_0), \quad z_- = \min(z, z_0),$$

and $J_0$ is the zero-order Bessel function.

Thus, from Green's formula (21), noting the boundary conditions (12)–(15), (17)–(20) and the relationship between $\eta$ and $\phi$:

$$\bar{\eta}(s,x,y) = -\frac{s}{g}\bar{\phi}(s,x,y,0), \quad (24)$$

we obtain the wave field:

$$\eta(t,x,y) = \frac{1}{\pi}\int_0^t \mathrm{d}\tau \int_{-\infty}^\infty \mathrm{d}x_0 \int_{-h}^0 \mathrm{d}z_0 \int_0^\infty f(t-\tau, x_0, z_0)\cos(gk\tanh kh)^{1/2}\tau \times \frac{\cosh k(z_0+h)}{\cosh kh} kJ_0(k((x-x_0)^2+y^2)^{1/2})\,\mathrm{d}k. \quad (25)$$

Therefore, the wave field is uniquely determined by the normal velocity distribution specified at the plane $y = 0$. In solving our problem, there is no other restriction upon the form of the integrable function $f(t,x,z)$ – the disturbance pattern can be either a simple oscillation across the plane or a disturbance pattern moving in the plane. Hence (25) is a fairly general expression for the wave field generated by disturbances specified at the vertical plane. It may be used to investigate various surface wave generation problems, either by turbulence or by a wavemaker. Also we notice that the contributions of the sources to the wave field decay exponentially with depth so that, as one would expect intuitively, the most important contributions come from the sources near the water surface.

For deep water, $h \to \infty$, (25) becomes

$$\eta(t,x,y) = \frac{1}{\pi}\int_0^t \mathrm{d}\tau \int_{-\infty}^\infty \mathrm{d}x_0 \int_{-\infty}^0 \mathrm{d}z_0 \int_0^\infty f(t-\tau, x_0, z_0) \times \cos(gk)^{1/2}\tau\, k\exp(kz_0) J_0(k((x-x_0)^2+y^2)^{1/2})\,\mathrm{d}k. \quad (26)$$

Next we investigate two simple cases which are relevant to wave generation by ship's turbulent wakes. The first case is related to the wave generation at the edges of small defect wake, where the velocity fluctuations at the edges may be viewed as harmonic motion. The second case is related to the wave generation at the edge of strong turbulent jets embedded in the small wake, where the velocity fluctuations may be

viewed as moving disturbances which are being regenerated and diminishing. In the forthcoming discussion, we will be only concerned with a single mode; the more complicated case can be studied via Fourier synthesis.

*Case 1. Waves generated by simple harmonic motion*

Suppose that the disturbance along the boundary is in a simple harmonic motion; that is, the normal velocity at each point in the plane oscillates with the same frequency $\omega$ ($\omega$ is constant), but its intensity $u(x, z)$ at the point does not change with time though it may vary with $x, z$:

$$f(t, x_0, z_0) = u(x_0, z_0) \sin \omega t \quad (t > 0). \tag{27}$$

Let $2l$ be the length of the source:

$$u(x_0, z_0) \neq 0 \quad \text{for } x_0 \in (-l, l),$$
$$u(x_0, z_0) = 0 \quad \text{otherwise.}$$

The waves generated by this velocity distribution at $y = 0$ of course have the same frequency $\omega$; $u(x_0, z_0)$ is a slowly varying function with respect to $x$ in the sense that

$$\frac{\partial u}{\partial x_0} \ll \frac{\omega^2}{g} u. \tag{28}$$

Let

$$\tilde{u}(x_0, k) = \int_{-\infty}^{0} u(x_0, z_0)\, k \exp(k z_0)\, \mathrm{d}z_0, \tag{29}$$

and assume $\tilde{u}(x_0, k)$ being a bounded function for the complex variable $k$. Therefore, according to (26), the wave field generated by the disturbance is

$$\eta(t, x, y) = \frac{1}{\pi} \int_0^t \mathrm{d}\tau \int_{-\infty}^{\infty} \mathrm{d}x_0 \int_0^{\infty} \tilde{u}(x_0, k) \sin \omega(t - \tau) \times \cos (gk)^{1/2} \tau J_0(k((x - x_0)^2 + y^2)^{1/2})\, \mathrm{d}k, \tag{30}$$

where $k$ essentially is the wavenumber. In this paper, we are only interested in the 'far field' where

$$k((x - x_0)^2 + y^2)^{1/2} \gg 1. \tag{31}$$

By applying the method of stationary phase to (30), we can show that, in the near field, $(x^2 + y^2)^{1/2} \ll 2l$,

$$\eta(t, x, y) = \frac{2}{\omega} \tilde{u}(x, \omega^2/g) \sin\left(\omega t - \frac{\omega^2}{g} y\right) \quad \text{as } \frac{\omega^2}{g} y \gg 1. \tag{32}$$

This represents parallel beams radiating away in the direction perpendicular to the plane, and their intensities do not change with distance from the plane.

At distances far away from the plane such that lengthscale of the source is much less than the distance, $R = (x^2 + y^2)^{1/2} \gg 2l$, the waves behave like radiation from a compact region.

$$\eta(t, x, y) = \mathrm{Im}\left\{\left(\frac{2}{\pi}\right)^{1/2} \frac{\omega}{g} \frac{2\pi}{(\omega^2/g\,R)^{1/2}} \tilde{U}\left(\frac{\omega^2}{g} \frac{x}{R}, \frac{\omega^2}{g}\right) \exp(\mathrm{i}(\omega t - \omega^2/gR + \pi/4))\right\}$$
$$\text{as} \quad \frac{\omega^2}{g} R \gg 1, \tag{33}$$

where $$\tilde{U}(m,k) = \frac{1}{2\pi}\int_{-\infty}^{\infty} \tilde{u}(x_0,k)\exp(\mathrm{i}mx_0)\,\mathrm{d}x_0.$$

Note the wave in the far field has a directional dependence on $x/R$. According to Fourier theory, $\tilde{U}(m,\omega^2/g)$ must tend to zero as $ml$ becomes very large so that the wave energy $\tilde{U}^2(m,\omega^2/g)$ is mainly concentrated in $m \leqslant O(1/l)$. Therefore, for non-compact sources, $l \gg \omega^2/g$, i.e. the lengthscale of the source is much larger than the waves, the wave radiate in a narrow fan-shaped region. For a compact source, $l \ll \omega^2/g$, i.e. wavelength is much larger than the lengthscale of the source, the wave beams spread in wider angles. For a point source, the waves spread uniformly in all directions in the $(x,y)$ half plane.

Therefore, the wave field generated by a simple oscillating disturbance consists of parallel beams with propagating direction perpendicular to the plane for distances not too far away from the plane and then spread out in the far field into a fan-shaped region. This redistribution of energy involves no change in the energy flux, and the energy flux radiated away by the waves is equal to the rate of working done by the pressure field on the fluid at the boundary (Gu 1989).

Generally, the intensity of the disturbances at the edge of defect wake is changing with time because of the decay of turbulence. If the timescale of variation of intensity is much larger than that of the oscillating motions of the boundary, we can generalize the calculation to include this slow variation effect. The normal velocity distribution along the boundary of a simple harmonic motion with a slow variation intensity may be written as

$$f(t,x,z) = u(x,z,\epsilon t)\sin\omega t, \tag{34}$$

where $\epsilon$ is a small parameter. By substituting (34) and

$$u(x_0,z_0,\epsilon t) = \int_{-\infty}^{\infty} \bar{u}(x_0,z_0,\Omega)\exp(\mathrm{i}\epsilon t\Omega)\,\mathrm{d}\Omega, \tag{35}$$

into (26), we can show that, to the lowest order,

$$\eta(t,x,y) = \left(\frac{2}{\pi}\right)^{1/2}\frac{\omega}{g}\int_{-\infty}^{0}\mathrm{d}z_0\int_{-\infty}^{\infty}\frac{1}{(\omega^2/gr)^{1/2}}k_0\exp(k_0z_0)\,u\left(x_0,z_0,\epsilon\left(t-\frac{r}{c_g}\right)\right)$$
$$\times\sin\left(\omega t-\frac{\omega^2}{g}r+\frac{\pi}{4}\right)\mathrm{d}x_0, \tag{36}$$

$$\text{as}\quad \frac{\omega^2}{g}r = \frac{\omega^2}{g}((x-x_0)^2+y^2)^{1/2} \gg 1 \quad (t\to-\infty),$$

where $k_0 = \omega^2/g$ is the wavenumber, and $c_g = g/2\omega$ is the group velocity of the waves. Hence for the near field $y \gg 2l$,

$$\eta(t,x,y) = \frac{2}{\omega}\int_{-\infty}^{0} u(x,z_0,\epsilon(t-y/c_g))\,k_0\exp(k_0z_0)\,\mathrm{d}z_0\sin(\omega t-k_0y). \tag{37}$$

For the far field $R = (x^2+y^2)^{1/2} \gg 2l$,

$$\eta(t,x,y) = \left(\frac{2}{\pi}\right)^{1/2}\frac{\omega}{g}\frac{2\pi}{(\omega^2/gR)^{1/2}}$$
$$\times\mathrm{Im}\left\{\int_{-\infty}^{0}\tilde{U}\left(\frac{\omega^2}{g}\frac{x}{R},z_0,\epsilon\left(t-\frac{R}{c_g}\right)\right)k_0\exp(k_0z_0)\,\mathrm{d}z_0\exp(\mathrm{i}(\omega t-\omega^2/gR+\pi/4))\right\} \tag{38}$$

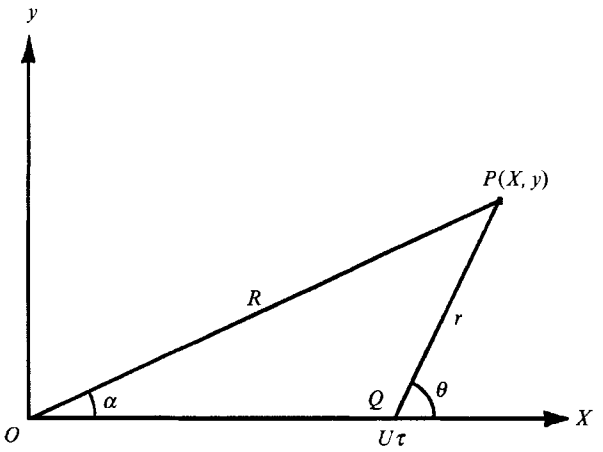


FIGURE 3. Notation for case 2 in §2.

where $$\tilde{U}\left(m, z_0, \epsilon\left(t-\frac{R}{c_g}\right)\right) = \frac{1}{2\pi}\int_{-\infty}^{0} u\left(x_0, z_0, \epsilon\left(t-\frac{R}{c_g}\right)\right)\exp(imx_0)\,\mathrm{d}x_0. \tag{39}$$

Comparing equations (37)–(38) with (32)–(33), we find that the geometrical characteristics of the waves generated by disturbances of changing intensity are the same as those of constant intensity: parallel beams in the distance, not too far away from the boundary, which spread into a fan-shaped region in the far field. The equations (37)–(38), however, exhibit a time-lag $y/c_g$ in the near field and $R/c_g$ in the far field, which is needed for the information about changes of intensity along the boundary to travel to the observation point $(x, y)$ at the wave group velocity.

*Case 2. Waves generated by moving disturbances which are being regenerated and diminishing*

When a turbulence jet is generated by a ship's propellers, the envelopes of the disturbances move with the ship, while the individual disturbances, whose intensities decay with time, move at the velocity different from that of the ship, with direction of the mean velocity of the jet being opposite to that of the ship. Here we consider one single mode of the disturbance $\cos Mx_0$ moving in the direction of the positive $x$-axis with constant velocity $V$, but its envelope $F(x_0, z_0)$ moving in the direction of the negative $x$-axis with constant velocity $U$:

$$f(t, x_0, z_0) = F(x_0 + Ut, z_0)\cos M(x_0 - Vt) \quad (t > 0), \tag{40}$$

with $U/V \geqslant O(1)$.

We again, at $t = 0$, assume

$$F(x_0, z_0) \neq 0 \quad \text{when } x_0 \in (-l, l),$$
$$F(x_0, z_0) = 0 \quad \text{otherwise,}$$

and define

$$G(x_0, k) = \int_{-\infty}^{0} F(x_0, z_0)\exp(kz_0)k\,\mathrm{d}z_0, \tag{41}$$

which is assumed to be a bounded function of $k$ in the complex plane. If we fix the reference on the moving envelope (figure 3):

$$X_0 = x_0 + Ut, \quad X = x + Ut,$$

and let $$W = U+V, \quad P_0 = X_0 - U\tau,$$

from (26) we have

$$\eta(t,x,y) = \frac{1}{\pi}\int_0^t \mathrm{d}\tau \int_{-l}^{l} \mathrm{d}P_0 \int_0^\infty G(P_0,k)\cos(gk)^{1/2}\tau \times \cos M(P_0 - W(t-\tau))\, J_0(k(x-U\tau-P_0)^2+y^2)^{1/2})\,\mathrm{d}k. \quad (42)$$

Applying the stationary phase method to the above integrals, we can obtain the wave field for $r = ((X-U\tau)^2+y^2)^{1/2} \gg l$

$$\eta(t,X,y) = 2\left(\frac{2\pi}{r}\right)^{1/2} \frac{\mathrm{Re}\,[\mathrm{i}\tilde{G}(0,k_0)\exp(-\mathrm{i}(k_0 r - MW\tau_0))\exp(-\mathrm{i}MWt)\exp(\pm\mathrm{i}\pi/4)]}{g^{1/2}(|1+4(U/V)^2(1-\frac{1}{2}\tan^2\theta)+4(U/V)|)^{1/2}}, \quad (43)$$

provided $$k_0\cos\theta = M, \quad (44)$$

where $$\tau_0 = \frac{2MVr}{g}, \quad c_g = \frac{g}{2MV}, \quad (45)$$

$\omega$ is the intrinsic frequency of the waves generated by disturbance, and

$$\tilde{G}(0,k_0) = \frac{1}{2\pi}\int_{-l}^{l} \mathrm{d}x_0 \int_{-\infty}^{0} F(x_0,z_0)\,k_0\exp(k_0 z_0)\,\mathrm{d}z_0. \quad (46)$$

Hence the wave appearing at point $P(X,y)$ at time $t$ is generated at time $t-\tau_0$. The wave intrinsic frequency is $MV$, the same as the frequency created by individual disturbance moving with velocity $V$ against the irrotational flow, and apparent frequency of waves is

$$n = \omega - \boldsymbol{k}\boldsymbol{U} = MW.$$

From (44) and (45) we have $c = V\cos\theta$, where $c$ is the phase velocity of the waves which determines wave propagation direction. The propagation direction is determined by the moving velocity of the patterns $V$ (the 'eddies') but not the velocity of the envelope $U$ (the ship). The term $\exp(-\mathrm{i}MWt)$ comes from the unsteady appearance of the disturbance in the moving frame of speed $U$. The amplitude of the waves is proportional to $\tilde{G}(0,k_0)$. It is the sum of the intensities of all points in the plane but weighted by factor $k_0\exp(k_0 z_0)$, and it decays like $1/r^{1/2}$. At

$$\theta^* = \arctan\left(\frac{1}{\sqrt{2}}\frac{1+2(U/V)}{(U/V)}\right), \quad (47)$$

the denominator in (43) becomes zero so that $\theta^*$ divides the waves into two classes. For $0 \leqslant \theta < \theta^*$, the waves belong to the transverse system, the sign in front of $\mathrm{i}(\pi/4)$ is positive; for $\theta^* < \theta \leqslant \pi/2$ the waves belong to the diverging system, the sign in front of $\mathrm{i}\pi/4$ is negative. When eddies are moving slowly relative to the envelope, $U/V \gg 1$,

$$\theta^* = \arctan\sqrt{2} \approx 54°\,44'. \quad (48)$$

At these critical angle, the amplitude decays like $1/r^{1/3}$, more slowly than what we found elsewhere.

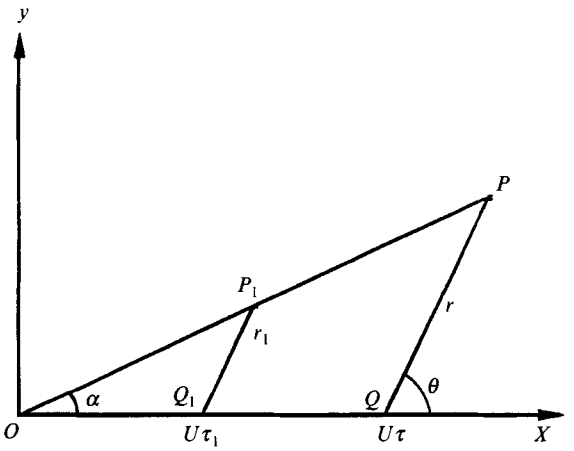


FIGURE 4. Notation for case 2 in §2.

From figure 4 we find that the waves generated during the time interval $(0, t)$ are all located along the line $OP$ in the frame fixed on the moving envelope since

$$\frac{r_1}{\tau_1} = \frac{r}{\tau} = c_g. \tag{49}$$

Therefore, $\alpha$, the angle between $OP$ and the $X$-axis, solely determines the location of waves relative to the moving envelope for the fixed wave frequency. From figure 4 we see that

$$\tan\alpha = \frac{r\sin\theta}{U\tau + r\cos\theta}. \tag{50}$$

Thus

$$\alpha = \arctan\frac{(c/V)(1-(c/V)^2)^{1/2}}{2(U/V)+(c/V)^2} \quad \text{or } \alpha = \arctan\frac{\sin\theta\cos\theta}{2(U/V)+\cos^2\theta}. \tag{51}$$

## 3. Narrow V-like ship wakes

In this section we will investigate the generation mechanism of backscatters in the bright arms by applying the results in the last section, where a wave field generated by a single mode of disturbances along the boundary has been studied in detail. Narrow V-like ship wakes detected by SAR have three distinguishing characteristics. (i) The half angle of the bright arms is very small, about 2° to 3°, and it depends on the ratio of group velocity of the backscatters to the ship speed. (ii) Backscatters in the bright arms are presumably short waves, whose wavelength $\lambda_s$, about 30 cm for L-band radar, satisfies the first-order Bragg scattering condition

$$\lambda_s = \frac{\lambda_r}{2\sin\theta_r},$$

where $\theta_r$ is the radar incident angle, and $\lambda_r$ is radar wavelength. (iii) The waves which form the backscatters in the bright arms are propagating along the same line that the radar is looking at, but the directions in which they are propagating are opposite in the two arms.

Lyden *et al.* (1988) found that the narrow V-like wakes often occur under light wind

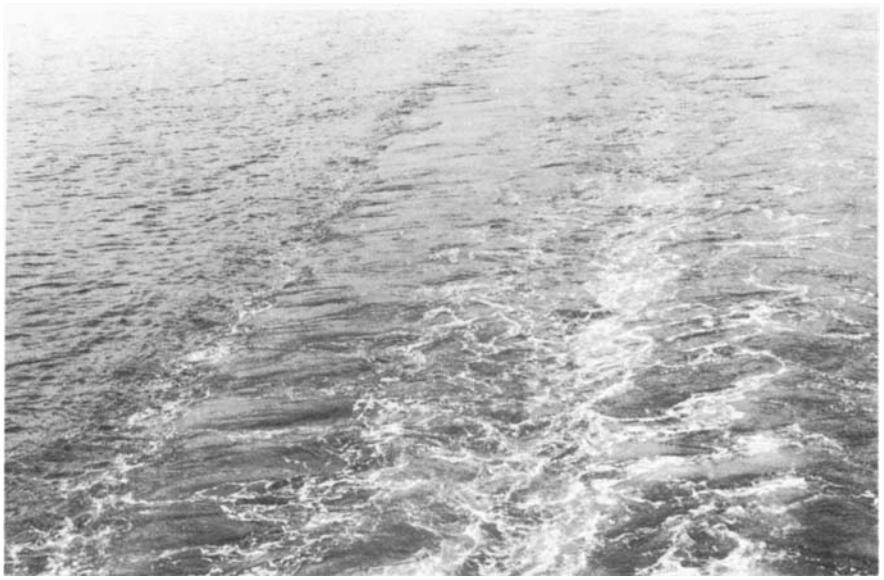

FIGURE 5. Downstream view of wave–wake system along the ship track.

conditions ($< 3$ m s$^{-1}$) for L-band radar and were apparently independent of any stratification of the water. Shemdin (1987, 1990) found from the measurements that the decay rate of the backscatters along the bright arms follows the combined effects due to molecular viscous damping and radiative decay.

In order to understand the generation mechanism, we believe that observations must be made of the turbulent wake immediately astern of the ship. A series of picture has been taken of the turbulent wakes during the ship *Bay Lady's* two-hour cruise at Baltimore Harbour in November 1988. The ship is 140 feet long and 40 feet wide. The wind speed was about 3 m s$^{-1}$, and the water surface was very calm in the bay and became a little rough when the ship reached Fort McHenry. The cruise velocity of the ship is about $6 \sim 8$ knots ($3$ m s$^{-1} \sim 4$ m s$^{-1}$) and the maximum speed of the ship is about 12 knots.

In this observation we found that the ship's turbulent wake near the ship's stern consists of two regions: one is the small defect wake generated by the ship's hull drag and full of swirling eddies, and the other is a strong jet generated by the propeller running through the middle of the small defect wake (figure 1). The turbulent intensity and mean velocity of the small defect wake are much smaller than that of the jet, and the lengthscale of the eddies is about 1 m or so. The jet runs in the opposite direction of the ship with respect to the undisturbed water, and waves are radiated away at the edges of the jet.

Figure 2 was taken of a region not too far from the ship's stern ($< 30$ m). It shows that the small-scale waves about 30 cm or so were generated and radiated away by the oscillating motion of the boundary between the turbulent wake and irrotational flow induced by the swirling eddies. Figure 5 is a broad view of the turbulent wake downstream. The small-scale wave region is perceptible along the boundary between the turbulent wake region and irrotational flow, and it persists for a long time after the ship has passed by.

These findings suggest that, under light wind conditions and moderate ship speeds ($3$ m s$^{-1} \sim 4$ m s$^{-1}$), the backscatter in the bright arms could be generated by the

boundary disturbance induced by swirling eddies in the ship wake not far away from the ship stern. We believe this should also be true for higher ship speeds.

The narrow V-like signatures observed in the SAR image are believed to be due to Bragg-scattering of radar waves by small-scale surface waves. The backscattering cross-section per unit area is given by the well-known formula

$$\sigma_0 = 4\pi k_r^4 \cos^4\theta_r F_1(\theta_r)\, \Phi(2k_r \sin\theta_r, 0). \tag{52}$$

That is, for a given radar wavenumber $k_r$ and incident angle $\theta_r$, the backscattering cross-section per unit area is linearly proportional to the surface wave spectrum $\Phi$ at wavenumber $2k_r \sin\theta_r$. To understand the behaviour of the wave spectrum $\Phi$, we utilize the idealized model discussed in §2. We take a control surface of the turbulent region as a vertical plane in which the normal velocity is prescribed, and the waves are generated by the disturbances along the control surface induced by the velocity and pressure fluctuations in the turbulence region.

The relationship between irrotational motion in the control surface and vortical motion in turbulence is very complicated. When strong turbulence impinges upon a free surface, the surface displacements are strongly coupled with the underlying vortical field and their propagation characteristics are disrupted, especially for scales of surface disturbance whose group velocity is not large compared with the turbulent velocities. It is very difficult to carry out a theoretical investigation of these processes since the mechanisms for the generation, scattering, and dissipation of the waves in turbulent flow have not been understood yet. We expect that, however, the irrotational fluctuations along the boundary may be mainly produced by two mechanisms: (*a*) direct induction by the coherent structures embedded in the turbulence (may be called 'direct mechanism') as in the case of no free surface (Phillips 1955), and (*b*) wave propagation from the inside of the turbulent region which is also generated by the coherent structures (may be called 'indirect mechanism'). In this investigation, we are more concerned about the wave propagation characteristics so we will prescribe the normal velocity along the control surface, leaving the quantitative relationship between the irrotational motion along the control surface and the vortical motion in the turbulence to be resolved by future experiments and observations.

In figure 1 we see that the strong jet rushing through the middle of the small defect wake can generate waves across the wake. The generation of these waves by the jet, which is a moving disturbance that are being regenerated and diminishing, has been discussed in detail in case 2 of §2. We can take a control surface of the jet, which separates the region of strong turbulence in the jet and the regions of weak turbulence in the small defect wakes, and then use (43) to calculate the wave spectrum generated by the jet with a range of scales of disturbances and advective velocities. In our observation, however, only those waves with wavelength about 1 m or longer have survived from crossing the small defect wake. The waves shorter than 1 m presumably have been consumed by turbulence. The surviving waves are too long to be the backscatters for the L-band radar. Therefore, the generation of waves by the ship's jets in our observation cannot explain the existence of two bright arms of the narrow V-like wakes. Of course, this does not exclude the possibility that those waves with wavelength about 30 cm or so, under some circumstances, may survive from crossing the small defect wakes and become the backscatters in the two bright arms of V-like wakes. In such a case, the wave spectrum can be analysed in a similar way to the case of wave radiation from boundaries of small defect wakes that we will discuss in the next few paragraphs; thus, we will not pursue this case further.

In the remainder of this section, we investigate the wave generation mechanism

indicated by figure 2, where the waves are radiated from the boundaries of small defect wake. From figure 2 we see that coherent structures are aligned along the boundaries. These coherent structures can be viewed as eddies, and the irrotational velocity induced by them along the boundary are responsible for the generation of small-scale waves with wavelengths of about 30 cm. The eddies in figure 2 are convected slowly downstream with lengthscale about 1 m or so.

Now we take a control surface of the small defect wake. This control surface is a vertical plane and it separates the irrotational flow from the turbulence in the wake. One would expect that the normal velocities along the control surface, induced by the vortical motion in the eddies, also exhibit coherent structures: those induced by the same eddy are well correlated while those induced by different eddies are approximately uncorrelated. Thus, each eddy acts as an individual source of the waves. The normal velocity coherent structures are also convected downstream with the eddies and their lengthscales slowly increasing downstream. As the eddies evolve and decay, they lose their identity and the new eddies are generated with intensity smaller than the previous one. Therefore, the decay timescale $T_d$ of the normal velocity at the control surface is the same order of magnitude as the lifetime of the eddy, which may be represented by the integral timescale derived from the time correlation function measured following the eddy. The physical significance of the decay timescale $T_d$ is that only those eddies with their ages younger than $T_d$ are actively generating waves and may be mostly responsible for the generation of the backscatters in the bright arms.

Therefore, as a ship moves across the water surface, the new eddies are generated immediately astern while the old eddies are dying away downstream. The eddies within the distance $UT_d$ from the ship's stern are in their energetic stage and are mostly responsible for the generation of waves; thus, the disturbance induced in the control surface from the ship's stern to the distance $UT_d$ downstream by the ship wake as a whole can be considered as an 'integrated source' of the backscatters in the bright arms. Therefore, the generation of the backscatters in the bright arms can be viewed as an 'integrated source' 'moving' across the water which radiates waves away from it. Since generally we are interested in the waves far away from the ship, as a good approximation, the slow convective motion and slow variation of the lengthscale of the coherent structures can be neglected. From this simple model, we seek some non-dimensional parameters which will determine the characteristics of the waves generated by the wake and lead to the determination of the wave spectrum by experiments and observations.

From now on, we use term 'coherent structure' for the coherent structure of the normal velocity in the control surface unless otherwise indicated. Suppose that the ship is moving from right to left with speed $U$ and let $2l$ be the average length of each individual coherent structure within the 'integrated source'; then let $x_0^{t'}, \ldots, x_i^{t'}, \ldots, x_{N_0}^{t'}$ be the centre of each coherent structure at time $t'$ with $x_0^{t'}$ being the newest eddy at that time and $x_{N_0}^{t'} - x_0^{t'} = UT_d$, and also let them denote the corresponding eddies.

The eddy $x_j^{t'}$ was obviously generated at time

$$t_j = t' - \frac{2l}{U} j \quad (j = 1, 2, \ldots). \tag{53}$$

Assume that the statistical characteristics of each eddy are the same, then the normal velocity distribution along the control surface induced by eddy $x_j^{t'}$ can be written as follows:

$$f_j(x, z, t) = u(x, z, T_j) \quad (x \in (x_j^{t'} - l, x_j^{t'} + l), \quad T_j > 0) \tag{54}$$

$$= 0 \quad \text{otherwise}, \tag{55}$$

where
$$T_j = t - t_j, \tag{56}$$

is the time lapse after eddy $x_j^{t'}$ was generated (the age of the eddy). $u$ is considered the same for all coherent structures along the control surface. Equation (54) can also be written as

$$f_j(x,z,t) = \int \tilde{u}(x,z,\epsilon T_j;\omega)\exp(\mathrm{i}\omega T_j)\,\mathrm{d}\omega \quad (x\in(x_j^{t'}-l, x_j^{t'}+l), \quad T_j>0), \tag{57}$$

where $\epsilon$ is a small parameter which accounts for the decay process of the eddy. For a single mode:
$$f_{j\omega}(x,z,t) = \tilde{u}(x,z,\epsilon T_j;\omega)\,\mathrm{d}\omega\exp(\mathrm{i}\omega T_j), \tag{58}$$

the wave field radiated away from the boundary is:

$$\eta_\omega(t,x,y) = \sum_j \left(\frac{2}{\pi}\right)^{1/2}\frac{\omega}{g}\int_{-\infty}^{0}\mathrm{d}z_0\int_{-\infty}^{\infty}\frac{k_0\exp(k_0 z_0)}{(k_0 r)^{1/2}}\tilde{u}\left(q,z_0,\epsilon\left(T_j-\frac{r}{\frac{1}{2}g/\omega}\right);\omega\right)$$
$$\times\exp(\mathrm{i}(\omega T_j - k_0 r+\pi/4))\,\mathrm{d}q\,\mathrm{d}\omega \quad (k_0 r\gg 1) \tag{59}$$

where
$$r=((x-q)^2+y^2)^{1/2}, \quad k_0=\frac{\omega^2}{g}. \tag{60}$$

Since the normal velocities along the control surface induced by the same eddy are well correlated, and since the depth of turbulent wake is much larger than the wavelength concerned here, it is a good approximation to assume that $u$ is independent of $z$.

Now define the wave spectrum observed at point $(x,y)$ and time $t$ as

$$\Phi(\omega;x,y,t) = \frac{\overline{\eta_\omega(t,x,y)\,\eta_\omega^*(t,x,y)}}{\mathrm{d}\omega}, \tag{61}$$

then, in the near field $y\ll 2l$, waves are parallel beams propagating outwards, and

$$\Phi(\omega;x,y,\epsilon t)\,\mathrm{d}\omega = \frac{4}{\omega^2}\overline{\tilde{u}(x,\epsilon\hat{T}_j;\omega)\,\mathrm{d}\omega\,\tilde{u}^*(x,\epsilon\hat{T}_j;\omega')\,\mathrm{d}\omega'} \tag{62}$$

if $x\in(x_j^{t'}-l, x_j^{t'}+l)$. Where

$$\hat{T}_j = T_j - \frac{y}{(g/2\omega)}. \tag{63}$$

Because wave group velocity is larger for the longer waves, the shorter waves are left behind the longer one; and because the intensity of turbulence in an eddy decreases with time, the weaker one is behind the stronger one for those waves of same wavelength. This is what figure 2 shows. The observed crest lines of the waves are not straight as theory would predict because the actual boundary between eddies and irrotational flow is not a perfect flat plane, but convoluted.

As wave propagate away from the wake, they soon reach the far field. When $y\gg 2l$, the wave is in the far field with respect to any eddy $x_j^{t'}$ so that

$$\eta_\omega(t,x,y) = \left(\frac{2}{\pi}\right)^{1/2}\frac{\omega}{g}\sum_j\int_{-l}^{l}\frac{\exp(\mathrm{i}(\omega T_j - k_0\rho_j^{t'}+\pi/4))}{(k_0\rho_j^{t'})^{1/2}} * \tilde{u}\left(q,\epsilon\left(T_j-\frac{\rho_j^{t'}}{\frac{1}{2}g/\omega}\right);\omega\right)\mathrm{d}q\,\mathrm{d}\omega, \tag{64}$$

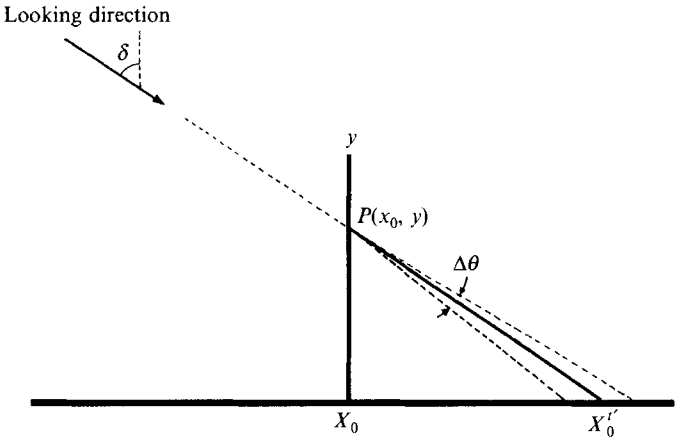


FIGURE 6. Thickened line: the boundary between turbulent wake and irrotational flow. $P(x_0, y)$ is the observation point, $Px_0'$ is the line along the radar looking direction, $\Delta\theta$ is the angular resolution of the radar.

where $$\rho_j^{t'} = ((x - x_j^{t'} - q)^2 + y^2)^{1/2}.$$

Now we define the correlation function of the normal velocity $u(x, t)$ in any particular coherent structure $x_j^{t'}$ as

$$Z(x, r; t, \tau) = \overline{u(x+r, t+\tau)\, u(x, t)} \quad x \in (x_j^{t'} - l, x_j^{t'} + l). \tag{65}$$

$Z$ is measured in a frame moving with the coherent structure along the control surface, and Fourier transform of $Z$ with $r$ and $\tau$ is

$$Z(x, r; \epsilon t, \tau) = \int_m \int_\omega \Upsilon(x, m; \epsilon t, \omega) \exp(imr) \exp(i\omega\tau)\, dm\, d\omega. \tag{66}$$

Since we assume that the velocities in the different coherent structures are not correlated, we obtain the wave spectrum:

$$\Phi(\omega; x, y, \epsilon t) = \sum_i \frac{8l\omega^2}{g^2} \frac{1}{k_0 r_i^{t'}} \Upsilon(x_*, k_0 p_i^{t'}; \epsilon \tilde{T}_i, \omega), \tag{67}$$

where

$$p_i^{t'} = \frac{x_i^{t'} - x}{((x - x_i^{t'})^2 + y^2)^{1/2}}, \quad \tilde{T}_i = T_i - \frac{((x - x_i^{t'})^2 + y^2)^{1/2}}{g/2\omega}, \quad r_i^{t'} = ((x - x_i^{t'})^2 + y^2)^{1/2}. \tag{68}$$

At any point $P(x, y)$ in the far field, the wave spectrum consists of waves propagating in different directions. The term under the summation sign in (67) represents the energy density radiated away by eddy $x_i^{t'}$ in the direction

$$\left( \frac{x_i^{t'} - x}{((x_i^{t'} - x)^2 + y^2)^{1/2}}, \frac{y}{((x_i^{t'} - x)^2 + y^2)^{1/2}} \right). \tag{69}$$

It is obvious that not all these waves can be 'seen' by the radar. If the angular resolution of the radar about wave direction is $\Delta\theta$, only those waves propagating along within the two dashed lines around radar-looking direction $\delta$ can make a contribution to the intensity of radar return (see figure 6). We let $\Phi_\delta(\omega)$ be the wave spectrum which consists of only those waves in the spectrum $\Phi(\omega; x, y, \epsilon t)$ that can be see by the radar

at the looking direction $\delta$. $\Phi_\delta(\omega)$ can be obtained from (67) by selecting only those waves propagating in the appropriate direction. However, the (67) is not convenient for practical applications. In order to interpret the SAR image of the ship wake, we need to simplify (67) to obtain a relation between the wave energy spectrum in the radar-looking direction and the parameters of the ship wake. Next we search for the non-dimensional parameters that determines the wave spectrum.

Suppose that the waves in the radar-looking direction $\delta$ appearing at a particular point $P(x_0, y)$ were generated by an 'integrated source' around time $t'$ at $x_0^{t'}$ on the boundary (figure 6). It is obvious that the first parameter is

$$N_0 = \frac{UT_d}{2l}, \tag{70}$$

which is the total number of terms in (67) that have to be summed since a major contribution to the wave field comes from those eddies within the distance $UT_d$ from the ship stern.

Now let

$$R = ((x_0 - x_0^{t'})^2 + y^2)^{1/2}. \tag{71}$$

The intensity of the waves at $P$ is also determined by the age $\tilde{T}_i$ of each eddy $x_i^{t'}$ when it generates them:

$$\tilde{T}_i = T_i - \frac{((x_0 - x_i^{t'})^2 + y^2)^{1/2}}{g/2\omega}. \tag{72}$$

Note that

$$\sin\delta = \frac{x_0 - x_0^{t'}}{R}, \tag{73}$$

then

$$\tilde{T}_i = \tilde{T}_0 + \frac{2il}{U}\left(1 - \frac{U\sin\delta}{c_g}\right). \tag{74}$$

If $U\sin\delta/c_g \approx 1$, then the waves propagating in the looking direction $\delta$ ($\approx \arcsin(c_g/U)$, generally $< 5°$) at $P$ were generated by the sources with relatively the same age, the intensity of these waves should be larger than the intensities of wave generated by the sources with quite different ages. Therefore, $U\sin\delta/c_g$ is the second parameters of the problem.

Let $R_c$ be the distance defined by

$$R_c \Delta\theta = UT_d. \tag{75}$$

For $R > R_c$, the 'integrated source' is well within the influence region so that the summation in (67) only need be carried out to the $N_0$th term. The further increase of $R$ does not cause the increase of the intensity of the total sources in the influence region so that for the far field $R > R_c \gg UT_d$, the wave spectrum falls approximately like $1/R$. For $R \ll R_c$, only part of the 'integrated source' is within the influence region. As $R$ increases, $R\Delta\theta$ increases, so does the influence region, and more and more terms in (67) have to be summed; therefore, the wave spectrum may vary much slower than $1/R$ along the looking direction. However, in the near field ($R \ll R_c$), $R\Delta\theta$ may only be a fraction of the length of the eddy, and the contribution to the wave field comes from only one eddy so that the wave spectrum still decreases as $1/R$. It is obvious that $R < R_c$ is satisfied near the ship where the waves have not propagated far. Thus, we should see a strong signal return from an area where the intensity of the wave field decreases as $1/R$ near the ship, and slower than $1/R$ at distances away from the ship if $N_0$ is large.

$R > R_c$ is satisfied at distances far away from the ship and waves are in the far field. Since the strongest wave energy is confined in a length $T_d c_g$ along the looking direction, we should see strong signal returns from a very narrow region. This is what we have found qualitatively in SAR images: two bright lines at a distance from the ship with scattering cross-section proportional to the inverse of the distance from the ship $1/X$ at $X < 0.5$ km, then varies slightly slower than $1/X$ at 0.5 km $< X <$ 4 km with some noise (Shemdin 1987, 1990). That is, the waves are continuously generated by the turbulence near the ship's stern as the ship moves forward, and propagate away being the backscatters in the bright arms.

Therefore, in the light of (67) and the discussion above, the wave spectrum in its nearly strongest region along the looking direction $\delta$ may be written as

$$\Phi_\delta(\omega) = \Psi_1(\pi_1, \pi_2, \pi_3) \frac{1}{k_0 R} \frac{2l\omega^2}{g^2} \Upsilon(x_*, k_0 \sin\delta; 0, \omega) \quad (y \gg 2l), \tag{76}$$

where

$$\pi_1 = \frac{UT_d}{2l}, \quad \pi_2 = \frac{U \sin\delta}{c_g}, \quad \pi_3 = \frac{R}{UT_d}. \tag{77}$$

The wavelengths of concern here are about 30 cm for L-band radar which have phase speed about 68 cm s$^{-1}$, group velocity 34 cm s$^{-1}$, and period of 0.44 s. $k_0 \sin\delta$ in $\Upsilon$ determines the directional spreading of the wave energy under the assumption that the boundary between turbulence and the irrotational flow is a plane. Since the real boundary generally is curved, $k_0 \sin\delta$ is not a good parameter to represent the directional spreading. It is better to leave the directional spreading to be determined by the observations. If we incorporate this effect into the function to be determined, (76) can be written as:

$$\Phi_\delta(\omega) = \Psi\left(\frac{UT_d}{2l}, \frac{U \sin\delta}{c_g}, \frac{R}{UT_d}\right) \frac{1}{k_0 R} \frac{2l\omega^2}{g^2} \Upsilon\left(0, \frac{\pi}{l}; 0; \omega\right), \tag{78}$$

with $\Psi$ being a function of three dimensionless parameters. The characteristics of $\Psi$ can be described as follows:

(i) $\Psi$ increases as $(UT_d/2l)$ increases since the available influence region increases. If $UT_d/2l$ is relatively small, say about one or two, $\Psi$ is approximately independent of $R$, and $\Phi_\delta$ decreases as $1/R$.

(ii) $\Psi$ is relatively large near the perpendicular looking direction ($\delta = 0$) and decreases as $\delta$ increases.

(iii) For $R \ll R_c$, $R\Delta\theta$ may only be a fraction of $2l$, the contribution comes only from one eddy so that $\Psi$ is independent of $R/UT_d$. Thereafter, if $UT_d/2l$ is large (say larger than 3), then $\Psi$ may increase as $R/UT_d$ increases until it reaches the value $R_c/(UT_d)$, then $\Psi$ remains constant if other parameters are fixed. Therefore, the wave spectrum decreases with distance as $1/R$ at distances not far away from the ship, slower than $1/R$ at intermediate distances if $UT_d/2l$ is large, and behaves like $1/R$ again in the far field $R > R_c$.

The characteristic (iii) agrees with observation as we have mentioned before. The characteristic (ii) also agrees with the observation that the strongest return signal occurs at a looking direction perpendicular to the ship track (Lyden *et al.* 1988). Since the small waves are propagating in various directions on both sides of the ship wake, and since they have the same statistical characteristics, the radar should be able to see waves on both sides of the wake with relatively the same strength. Therefore, the appearance of the narrow V-like wakes is consistent with the Bragg-scattering of radar

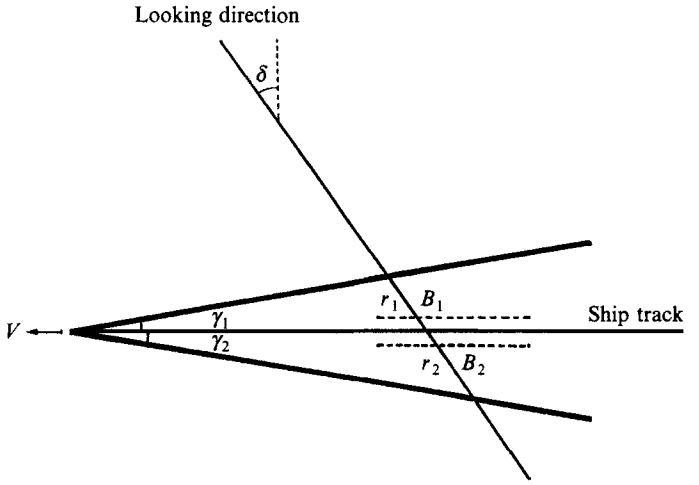


FIGURE 7. Thickened lines: the locations of the strongest backscatters. Dashed lines: boundaries between turbulent wake and irrotational flow. $B_1$ and $B_2$ are the intersection points of the boundaries with a line along a looking direction.

waves by small-scale surface wave generated by the boundary disturbance at the interface between turbulence and irrotational flow induced by turbulence in the ship wake near the ship stern. The dependence of $\Psi$ on the three parameters can be determined by experiments.

Now consider the angle of the bright arms. Let a line along the looking direction intersect two boundaries of the ship wake at $B_1$ and $B_2$ as shown in figure 7. Assume the width of the wake is $L$ which is slightly larger than the width of the ship. Then the eddy at $B_2$ was generated at time

$$\Delta T = \frac{L\tan\delta}{U}, \tag{79}$$

earlier than that at $B_1$. Assume $L_1$ is the distance that the ship has travelled after eddy $B_1$ has been generated. Then waves generated at $B_1$ and $B_2$ have travelled distances

$$r_1 = c_g\frac{L_1}{U}, \tag{80}$$

$$r_2 = c_g\frac{L_1 + L\tan\delta}{U}, \tag{81}$$

respectively. Thus, the half angles of the two arms with respect to the ship track are determined by

$$\tan\gamma_1 = \frac{r_1\cos\delta + 0.5L}{L_1 - r_1\sin\delta}, \tag{82}$$

$$\tan\gamma_2 = \frac{r_2\cos\delta + 0.5L}{L_1 + L\tan\delta + r_2\sin\delta}. \tag{83}$$

At distances far away from the ship,

$$\frac{L}{L_1} \ll \frac{c_g}{U} \ll 1, \tag{84}$$

we have $$\tan\gamma_1, \quad \gamma_2 \approx \frac{c_g}{U}\cos\delta \tag{85}$$

which is consistent with the observation made by Shemdin (1987, 1990).

## 4. Concluding remarks

It has been demonstrated that the backscatters in the bright arms of narrow V-like ship wakes are short waves generated by the oscillating motion at the edges of the turbulent wake of the ship. The characteristics of the waves have been discussed in detail through an idealized model: waves are generated by velocity fluctuations, induced by turbulence, along a vertical control surface which separates irrotational flow from turbulence. The results can explain some of the observed features of narrow V-like wakes, such as the angle of the wake and the variation of the intensity of radar return with the distance away from the ship.

There are several other processes that may play some role in the narrow V-like ship wakes. So far we have considered only linear wave theory in this investigation. The nonlinear wave–wave interactions may become significant after a period of time, which results in modifications of the wave spectrum and redistribution of wave energy in various directions. However, the wave amplitudes decrease with time after waves are generated because of viscous damping and angular spreading of wave energy so that if the linear wave theory is assumed a good approximation for the problem at the very beginning of the wave generation, the nonlinear effects are negligible thereafter. Interaction between small-scale waves generated by turbulence and Kelvin ship-waves may occur too. From our observation, the Kelvin ship waves are present outside the region of small-scale waves and small-defect wake, and they propagate faster than the small-scale waves (cf. figure 2). Thus the interaction seems unlikely.

From a theoretical point of view, the waves may also be generated by eddies in the boundary layer along the ship's hull as suggested by Shemdin (1990). These waves were observed during the cruise when the ship had not reached its cruise speed but disappeared later, presumably being destroyed by the breaker generated by the ship near the stern. The ship *Bay Lady* is relatively shorter than most merchant ships. If the ship is long enough (as in Shemdin 1987), these waves may have the chance to propagate out before the breaker catches them.

D.G. would like to express his gratitude to Professor D. Strobel for his critical reading of the early draft, and to Dr Norden Huang and Professor C. C. Mei for many valuable discussions. This research is supported by the Office of Naval Research under contract N00014-84-K-0080.

## REFERENCES

GU, D. 1989 On surface wave generation by boundary disturbances. PhD dissertation. The Johns Hopkins University.

LYDEN, J. D., HAMMOND, R. R., LYZENGA, D. R. & SHUCHMAN, R. 1988 Synthetic aperture radar imaging of surface ship wakes. *J. Geophys. Res.* **93**, C10, 12293–12303.

MEI, C. C. 1983 *The Applied Dynamics of Ocean Surface Waves*. John Wiley.

MICHELL, J. H. 1898 The wave resistance of a ship. *Phil. Mag.* [5] **45**, 106–133.

MUNK, W. H., SCULLY-POWER, P. & ZACHARIASEN, F. 1987 Ships from Space. *Proc. R. Soc. Lond.* A **412**, 231–254.

PHILLIPS, O. M. 1955 The irrotational motion outside a free turbulent boundary. *Proc. Camb. Phil. Soc.* **51**, 220–229.

SHEMDIN, O. H. 1987 SAR imaging of ship wakes in the Gulf of Alaska. Final Rep. N00014-84-WRM-2212, Office of Naval Research, Arlinton, VA.

SHEMDIN, O. H. 1990 Synthetic aperture radar imaging of ship wakes in the Gulf of Alaska. *J. Geophys. Res.* **95**, c9, 16319–16338.

URSELL, F. 1966 On the rigorous foundation of short-wave asymptotics. *Proc. Camb. Phil. Soc.* **62**, 227–244.